



## BIOMEDICAL IMAGE FUSION USING DISCRETE WAVELET TRANSFORM

Ewelina SOBOTNICKA<sup>1</sup>, Monika RICHTER-LASKOWSKA<sup>1,2</sup>

<sup>1</sup> Łukasiewicz Research Network – Krakow Institute of Technology, The Centre for Biomedical Engineering, Krakow, Poland

<sup>2</sup> Institute of Physics, Faculty of Science and Technology, University of Silesia in Katowice, Chorzow, Poland

**Source of support:** Own sources

**Author's address:** E. Sobotnicka. Łukasiewicz Research Network – Krakow Institute of Technology, Zakopianska Street 73, 30-418 Krakow, Poland, e-mail: ewelina.sobotnicka@itam.lukasiewicz.gov.pl

**Abstract:** Medical imaging involves creating images of physiological and pathological changes occurring in the human body using various types of specialized methods. The purpose of diagnostic imaging, among other things, is to assess the size, shape of the internal structure and function of various internal organs. There are no universal imaging methods that effectively combine anatomical, functional, or size and differentiation information of tissues or objects in the visualized image. Images obtained by the various imaging techniques reveal different types of diagnostic information. The post-processed images are displayed in a variety of dedicated tools that facilitate their interpretation. It is often the case that the image is displayed in different sequences, photo by photo. Unfortunately, situations arise where the first image differs from the previous one, and the structure analyzed in it is shifted. To prevent such phenomena, image fusion is carried out during processing. It guarantees to improve the quality of the information contained in the set (whole projection) of images of a given anatomical structure. The article is an attempt to discuss the application of the discrete wavelet transform in biomedical image processing. The main task of the ongoing work was to combine images from different sequences showing the same structure. As a result of pre-processing, images with high spatial resolution were obtained, which in further processing steps can be used to analyze the features of objects in the analyzed images.

**Keywords:** biomedical images, image fusion, discrete wavelet transform, image processing

**Figures:** 2 • **Table:** 1 • **References:** 15 • **Full-text PDF:** <http://www.pjambp.com> • **Copyright** © 2021 Military Institute of Aviation Medicine, ul. Krasieńskiego 54/56, 01-755 Warsaw, license WIML • **Indexation:** Index Copernicus, Polish Ministry of Science and Higher Education

## INTRODUCTION

Processed biomedical images are being used more and more often to analyze a patient's condition. The post-processed images are displayed in a variety of dedicated tools that facilitate their interpretation. Therefore, it is important that no degradation or loss of clinically important information contained in the image occurs during processing. Through the use of image fusion mechanisms, the relevant information in each image is merged into a single whole, creating the resulting image, the quality of which is often much better than images displayed separately. Image fusion methods include [1,7,8,10]:

- simple image fusion,
- pyramid decomposition,
- discrete wavelet transform.

With simple image fusion, it is possible to create direct image fusions using basic mathematical operations such as addition, averaging, subtraction, or, by skipping the pixel intensities of the analyzed input images [1,7,9]. Pyramidal decomposition, due to its simplicity, allows the image to be hierarchically divided into smaller and smaller parts and the features for each part to be determined [1,9]. Unfortunately, the use of simple operations for images with poor brightness and low contrast can cause an adverse reduction in contrast and readability of the analyzed image. In such a case, a discrete wavelet transform can be a helpful tool, whereby the image, as a result of decomposing each image of a given projection separately, is zoomed back and smoothed [1,7,8].

For biomedical images, legibility and the clinical information contained in the images must be as accurate as possible. Therefore, during processing, the relevant information contained in the image cannot be lost. Therefore, the paper presents the initial process of image fusion using the discrete wavelet transform method, which is considered one of the more accurate methods of image fusion [1,9,11].

## MEDICAL IMAGE FUSION

By default, Computed Tomography (CT) and Magnetic Resonance Imaging (MRI) are used to acquire medical images. With CT technology, anatomical information is displayed, but without information about the activity of the structure in question (for example, heart rate, flows in blood vessels) [2]. MRI technology, on the other hand, makes it possible to provide both information on the anatomy and activity of the structures under study [12,13,14]. Images produced by CT technol-

ogy have lower spatial resolution than those from MRI, so it is advisable to process them accordingly. The goal of image fusion is to obtain an image containing anatomical and functional information with very good, analyzable resolution [3,4,9,15]. This chapter discusses the basics associated with the discrete wavelet transform and its potential use in the process of combining biomedical image sequences. The image preprocessing process discussed here was carried out in the MATLAB environment, using dedicated functions contained in the Wavelet Toolbox.

### Discrete wavelet transform

The wavelet transform involves decomposing a signal and representing it as a linear combination of basis functions called wavelets [1,7,11]. It has applications in compression, signal de-noising or image fusion [5]. It is distinguished from other methods by multistage signal decomposition, variable resolution in the time and frequency domains, and the ability to use basis functions other than harmonic functions [1,5]. The discrete wavelet transform of the signal  $x(t)$  is determined as the dot product of  $x(t)$  and a sequence of basis functions  $\psi(t)$  [1]:

$$DWT = \int_{-\infty}^{+\infty} \psi(t) * x(t) dt$$

where

$\psi(t)$  – wave function,

$x(t)$  – tested signal dependent on time  $t$

The most commonly used wavelet is the so-called Haar wavelet, the basic form of which is expressed by the equation [1,5]:

$$\psi(t) = \begin{cases} 1 & \text{for } 0 \leq x < \frac{1}{2} \\ -1 & \text{for } \frac{1}{2} \leq x < 1 \\ 0 & \text{for others } x \end{cases}$$

The scaling function, on the other hand, is of the form:

$$\varphi(x) = \begin{cases} 1 & \text{for } 0 \leq x < 1 \\ 0 & \text{for others } x \end{cases}$$

The collection of fundamental wavelets used for signal analysis is numerous, still open, so they find applications in various fields of technical sciences [1]. Due to their wide application, they can also be used in medical image processing. Therefore, the paper attempts to implement the wavelet transform in the MATLAB environment

for image processing purposes. Calculations were performed using the Wavelet toolbox. Calculations performed in the MATLAB environment allow entropy to be determined. In order to obtain the optimal image after merging, it is necessary to decompose the image using wavelet packets, and then determine the entropy index for each set.

### Wavelet transform of biomedical images


















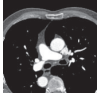

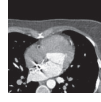
In general, it can be said that the wavelet transform involves the decomposition of an image into parts: approximating and detail elements (diagonal, vertical and horizontal) [5]. Thanks to the properties of the wavelet transform that allow it to be generalized to any dimension, it is possible to use it for multiresolution representation of images [1,5]. The essence of this process is the decomposition of the image into four components with a resolution twice smaller than that of the original image. Each image formed during decomposition can be divided into four more images in further stages of analysis [5]. The resulting image representation consists of multiple levels of resolution. During the decomposition process, low-pass and high-pass filtering of rows (R) and columns (C) occurs. Depending on the order as well as the type of filters, images are obtained, marked with the following symbols: HH – image after high-pass filtering for rows and columns, HL – image after high-pass filtering for rows and low-pass filtering for columns, and LL – image after low-pass filtering for rows and columns, LH – image after low-pass filtering for rows and high-pass filtering for columns.

### RESEARCH MATERIAL

For the purpose of testing, a database consisting of 40 medical images was created. The collection was separated into images produced by imaging structures related to the aorta (Patient A) and the coronary vessels (Patient B). For each patient, 20 images were selected for decomposition and then merged. The images used for analysis were from the European Society of Radiology's EURORAD Case Database [6]. The images used were from two series of CTA (Angiography Computed Tomography) scans. In the study of coronary vessels, the so-called Calcium Score (CaSc), a level of vascular calcification, was additionally analyzed, thus the images are stored in the database as CaSc. For the tests carried out, the level of calcification was not relevant therefore it was not analyzed. Because we had CaSc and CTA30% im-

ages from a single patient, they were included in the analysis as input data to test the decomposition and merging process. Examples of the image series used to carry out the merging process are placed in the table (Table 1). The table is divided into two main columns. The first column was for Patient One, designated as A. This column was divided into CTA30% (10 images) and CTA70% (10 images) images. That is, the images were from angiographic CT scans with dose levels of 30% and 70%. On the other hand, column two contains images from Patient 2 (labeled B). Here, the images were divided into 2 groups, which presented images formed during the study of coronary calcification (CaSc, 10 images) and images in which the dose level was reduced and amounted to 30% (10 images). The images did not indicate specific locations of the aorta or coronary vessels, as this was not the subject of the works carried out. The purpose of the works carried out was to obtain preliminary information on the effectiveness and suitability of using the wavelet transform to combine medical images, rather than to quantitatively analyze the features of the structures in them.

Tab. 1. Presentation of sample images used in the merging process.

Patient A		Patient B	
Structures of the aorta		Coronary vascular structures	
CTA 30%	CTA 70%	CaSc (Calcification Score)	CTA 30%
			
			
			
			
			

## RESULTS

The main objective of the ongoing work was to explore the possibility of using the wavelet transform to combine medical images from different sequences of the same examination. For this purpose, an image preprocessing methodology was developed in the MATLAB environment, consisting of several steps involving:

- creating a column vector of input images,
- calculating the covariance matrix of two columns,
- calculating the values and eigenvectors of the matrix,
- normalizing the column vector by multiplying each pixel of the image by the appropriate weights,
- compiling the two matrices to produce the final combination of images.

A discrete wavelet transform at the first level of resolution was used to perform image fusion during decomposition. It made it possible to detail the relevant information found in the image. During testing, high-pass and low-pass filtering was applied using the appropriate order of the matrix of coefficients. The matrix of wavelet coefficients tells how much a given signal overlaps with the wavelet being compared [1,5]:

$$C(\text{scale}, \text{position}) = \int f(t) * \psi(\text{scale}, \text{position}, t) dt,$$

where:

C – matrix of coefficients

f(t) – analyzed signal

$\psi$  (scale, position, t) – base wave.

In the initial phase of testing, the configuration of the matrix of coefficients took the form: for image one  $A^1L^1, H^1L^1, V^1H^2, D^1H^2$  and for image two  $A^2L^2, H^2L^2, V^2L^1, D^2L^1$ . Where A denoted the approximation factor falling in the range  $1 \leq i \leq N$  (N – integer number). And H, V and D stand for the corresponding matrix coefficients: horizontal, vertical and diagonal. Using the H, V and D components, it is possible to calculate parameters that characterize the edges of objects, along with imaging the distribution of structures contained in the image. The work was divided into two phases. The first phase involved loading two images showing the same structure (from different series) and performing their decomposition (Fig. 1a). The second phase, on the other hand, involved combining the images processed in the first phase (Fig. 1b). The results obtained are summarized in graphical form, which shows the original images, decomposed images and one resultant image that is a compilation of

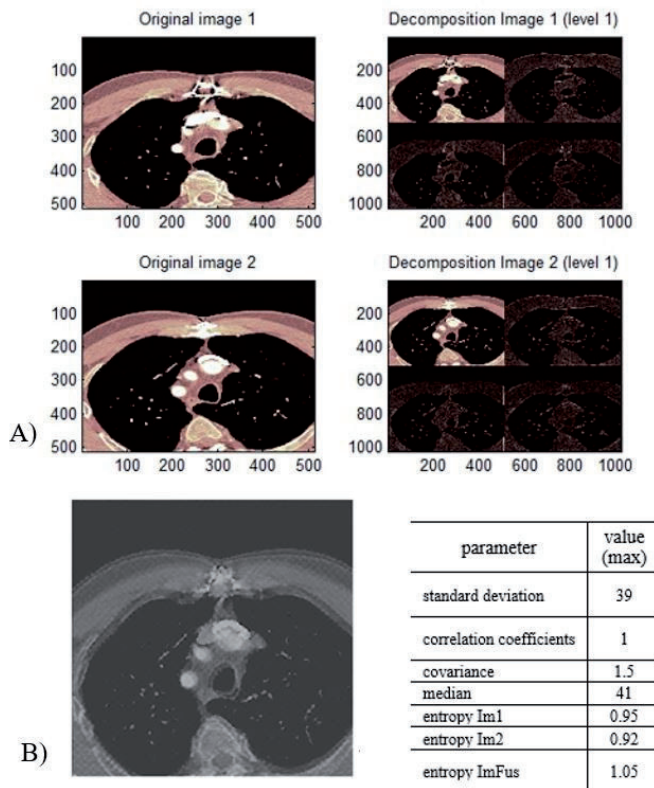


Fig. 1. Experiment I. Merging process performed on two images from Patient A. (A) decomposition phase, (B) resultant image of the merging phase and table with results for Experiment I.

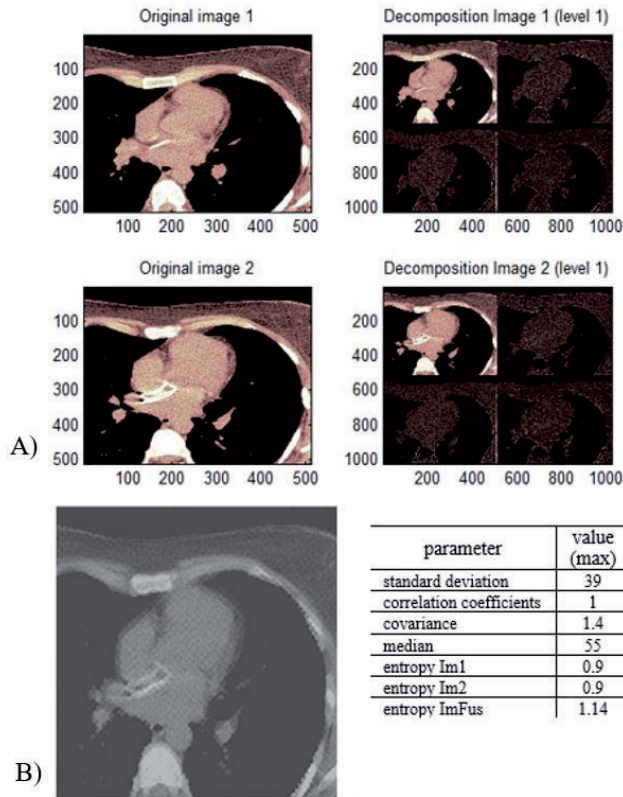


Fig. 2. Experiment II. The merging process performed on the first two images from Patient B, (A) the decomposition phase, (B) the resulting image of the merging phase, and a table with the results for Experiment I.

the first image (Original image 1) and the second image (Original image 2). To better illustrate the results, a table of the parametric dataset is placed next to the resulting image.

Similar work was carried out for the set of images of patient two. Images from projections during which the degree of coronary artery calcification (CaSc) was examined were analyzed. The performed works were also divided into two phases. The first phase involved loading two images showing the same structure (from different series) and performing their decomposition (Fig. 2a). The second phase, on the other hand, involved combining the images processed in the first phase (Fig. 2b). The results obtained are summarized in graphical form, which shows the original images, decomposed images and one resultant image that is a compilation of the first image (Original image 1) and the second image (Original image 2).

Standard image statistics were calculated using MATLAB functions to determine: standard deviation (std), correlation coefficient (corrcoef), covariance (cov), median (median) and entropy (entropy). A set of 20 images were used for the analysis, which were merged with each other. The merge resulted in 10 resultant images. The calculation of parameters such as standard deviation, cor-

relation coefficient, covariance and median pixel intensity, entropy of merged images was realized based on the resulting images, after the merging phase. The entropy value was also determined for single original images. The results, which are presented in Fig. 1 and Fig. 2, are for two sample experiments, out of the ten that were conducted. In this work, the standard deviation was determined to obtain information on the value of pixel intensities, as well as to estimate losses in the images after they were merged. The standard numerical measure of loss is usually the standard deviation of the pixel values of the reconstructed image from the original. However, the most important "measure" of loss assessment is the opinion of the observer. The fewer differences (or lack thereof) the observer detects, the higher the quality of the algorithm. The standard deviation in both analyzed cases is equal to the value of 39 and is clustered around the mean value of 46, which shows the high potential of the algorithm. Another parameter analyzed was the correlation coefficient between the original image and the same image processed with the median filter. The correlation coefficient in both cases was 1. This value demonstrates the strong relationship between the combined images. The covariance values obtained

differed slightly, in the first case analyzed (Fig. 1) it was 1.5, in the second (Fig. 2) it was 1.4. The values obtained are convincing of the positive correlation and interdependence between the images. The paper also determined the median pixel brightness, which was 41 in the first case and 55 in the second. These values denote the output intensity values of the pixels in the image, which can be useful information for further analysis. The entropy of the first image (entropy  $Im_1$ ), the second image (entropy  $Im_2$ ), and the merged images (entropy  $Im_{Fus}$ ) were also analyzed. Entropy results in the context of images can be used to characterize the texture of an image. Entropy determines the complexity of an image; the more detail that is visible in a texture, the higher the value this characteristic takes. The entropy value for the merged images from the first experiment is 1.05, while that from the second is 1.14. In both cases there was an increase in entropy values, with a slight increase for the first case analyzed. In experiment two (Patient B), we observe a shift in the image, which confirms the entropy value (1.14). However, the preliminary statistical analysis, at this stage of the work, gives satisfactory results and provides the basis and motivation for further research related to the development of the image fusion algorithm.

The merging phase yielded a resultant image with a high level of quality. The term quality means sharpness (pixel intensity). The method of merging images makes it possible to create different configurations of them, making it unnecessary to merge and visualize the entire series of images.

It is also possible to select for analysis only those images that contain relevant information for the user. In both cases presented above, the resulting image, which is a fusion of two intermediate images, can provide valuable information about the structure in question in further stages of analysis.

## CONCLUSIONS

Ongoing preliminary work on the feasibility of using the wavelet transform for merging biomedical images is showing promising results and may provide a rationale for further image processing work. The preliminary statistical analysis carried out and the results obtained prove the validity of the work carried out. The idea behind image fusion is to sharpen the information, which is not the case if the spatial structures in the original image are only slightly enhanced. The combination results in a high-resolution image, as evidenced by the standard deviation, correlation coefficient as well as the positive covariance score, among other things. The merged image sequences can be used in further processing steps, such as in segmentation, where already preprocessed images are used. The wavelet transform approach in preprocessing can become a helpful tool for proper image preparation for further processing steps related to separating structures that are difficult to see in images.

Algorithm improvements are being sought to achieve better visual quality with higher fusion rates.

## AUTHORS' DECLARATION:

**Study Design:** Ewelina Sobotnicka, Monika Richter-Laskowska. **Data Collection:** Ewelina Sobotnicka, Monika Richter-Laskowska. **Manuscript Preparation:** Ewelina Sobotnicka, Monika Richter-Laskowska. The Authors declare that there is no conflict of interest.

## REFERENCES

1. Białasiewicz JT. Falki i aproksymacje. Wydawnictwo Naukowo-Techniczne 2000.
2. Borzecki M, Skurski A, Balcerzak B, Kaminski M, Napieralski A, Kasprzak JD, Lipiec P. Image Processing Methods for Diagnostic and Simulation Applications in Cardiology. *International Journal of Microelectronics and Computer Science*. 2012; 146-151.
3. Chen M, Fu Y, Li D. Image fusion based on extensions of independent component analysis. *The International Archives of the Photogrammetry, Remote Sensing and Spatial Information Sciences*. 2008; 37: 1111-1118.
4. Dou W, Chen Y. An improved ihs image fusion method with high spectral fidelity. *The International Archives of the Photogrammetry, Remote Sensing and Spatial Information Sciences*. 2008; 37: 1253-1256.
5. Dwornik M. Analiza czasowo – częstotliwościowa. *Analiza i Przetwarzanie Sygnałów i Obrazów Cyfrowych*. Geoinformatyka 2020/2021.

6. Eurorad. Radiological Case Database. <http://www.eurorad.org/>, 2022.
7. Hamsalekha R, Rehna V. Analysis of Fusion Techniques with Application to Biomedical Images: A Review. *International Journal of Emerging Engineering Research and Technology*. 2015; 3: 70-78.
8. Klonus S, Ehlers M, Performance of evaluation methods in image fusion. 12th International Conference on Information Fusion, USA 2009; 1409-1416.
9. Kos A, Skalski A, Zielinski T. A modified ASM algorithm, that considers a CT and MRI medical data anisotropy at the stage of statisticshape model generation. *Przegląd Elektrotechniczny*. 2015; 5.
10. Krishnamoorthy S, Soman K. Implementation and Comparative Study of Image Fusion Algorithms. *International Journal of Computer Applications*. 2010; 9: 25-35.
11. Mulcahy C. Image Compression Using The Haar Wavelet Transform. *Spelman College Science & Mathematics Journal*. 1997; 1.
12. Przelaskowski A. Ocena jakości obrazów. In: *Multimedia - Algorytmy i Standardy kompresji* (red. W. Skarbek). Akademicka Oficyna Wydawnicza. 1998; 9: 154-183.
13. Sobotnicka E, Jeżewski J, Sobotnicki A. Metody segmentacji obrazów układu sercowo-naczyniowego do rozpoznawania blaszek miażdżycowych. W: *Inżynieria Biomedyczna. Podstawy i zastosowania* (red. Władysław Torbicz) and *Obrazowanie Biomedyczne* (red. Mariusz Kaczmarek, Leszek Królicki, Juliusz Lech Kulikowski, Antoni Nowakowski). Akademicka Oficyna Wydawnicza EXIT. Warszawa, 2020.
14. Tadeusiewicz R. *Informatyka Medyczna*. Instytut Informatyki UMCS. Lublin, 2011.
15. Zhang Y. Understanding Image Fusion. *Photogrammetric Engineering & Remote Sensing*. 2004; 657-661.

**Cite this article as:** Sobotnicka E, Richter-Laskowska M. Biomedical Image Fusion Using Discrete Wavelet Transform. *Pol J Aviat Med Bioeng Psychol* 2021; 27(1): 32-38. DOI: 10.13174/pjambp.28.02.2024.04